Biochimica et Biophysica Acta, 470 (1977) 161—169

BBA 77820

THE INTRINSIC STRUCTURAL ASYMMETRY OF HIGHLY CURVED PHOSPHOLIPID BILAYER MEMBRANES

ADELA CHRZESZCZYK, ARNOLD WISHNIA and CHARLES S. SPRINGER, Jr.
Department of Chemistry, State University of New York, Stony Brook, N.Y. 11794 (U.S.A.)
(Received April 12th, 1977)

Summary

Phosphorus-31 NMR studies of solutions of small L-α-dipalmitoyl phosphatidylcholine bilayer vesicles containing sodium dimethyl phosphate uniformly distributed between the continuous external and the intravesicular aqueous spaces, with the paramagnetic shift reagent Pr^{3+} present only in the external space, are reported. These studies give the distribution both of dipalmitoyl phosphatidylcholine in the vesicle inner and outer monolayers and of dimethyl phosphate in the aqueous spaces. With the third necessary parameter obtained from the vesicle sedimentation coefficient, the very different packing parameters of dipalmitoyl phosphatidylcholine in inner and outer monolayers can be determined. The vesicle outer radius is 109 Å. Although the total bilayer thickness is virtually identical to that of planar bilayers, the outer monolayer is thicker (20 Å) and the inner monolayer thinner (15 Å). The area per head group at the inner surface, 68 $Å^2$, is like the planar value, but the tails are much more folded, so as to decrease the radial lengths and increase the tangential spread (to 94 $Å^2$). The reverse is true in the outer layer: the surface per head group is 76 $Å^2$, tapering to 51 $Å^2$ in the tail region, so that outer layer tails are relatively extended. The difference is equivalent to a shift of about two 2g1 kinks from outer to inner layers; the uneven packing certainly affects fluidity, and may have important biological consequences.

Introduction

It is well known that there are biological membranes which exhibit regions of very small radius of curvature (perhaps as low as 75 Å). Examples include the membranes of the small neurotransmitter storage vesicles in the synaptic regions of neurons, the highly convoluted cristae of the mitochondrial inner membrane, the edges of retinal rod outer segments and disks and the brush borders of intestinal epithelial cells. Sheetz and Chan [1] have suggested that

the curvature itself would affect dynamic behavior (lateral diffusion, local motion) and equilibrium properties (trans-gauche conformer populations and their thermodynamic consequences). The first studies [2—4] of model systems showed large changes in conformer populations across the gel-liquid crystalline phase transition, but no major differences between planar and sharply curved bilayers. More recent work (Von Dreele, P.H. and Chan, S.I., unpublished work and refs. 5—10), however, has demonstrated detailed differences, particularly below the transition temperature. Raman, fluorescence and differential scanning calorimetry studies [5,8—10] show a difference in phase transition behavior between planar and curved bilayers, while nuclear (NMR) and electron (EPR) magnetic resonance and fluorescence studies (Von Dreele, P.H. and Chan, S.I., unpublished, and ref. 7), show differences in lateral phase separation of mixed lipid preparations during melting of the two kinds of bilayer. The profound effect of the physical state of a membrane on its biological function has recently been reviewed [11].

The underlying source of these effects is surely the intrinsic structural asymmetry of highly curved phospholipid bilayer membranes. In earlier work, paramagnetic transition metal and lanthanide ions have been used to separate the ^{1}H, ^{13}C, and ^{31}P NMR resonance lines of the phospholipid head groups of the inner and outer surfaces of bilayer vesicles (see ref. 12 for references). In this paper we will show how a logical extension of this approach, coupled with a hydrodynamic measurement, can be used to determine all the parameters required to characterize the basic geometric asymmetry of a spherical bilayer vesicle [12] (if the vesicle has lower symmetry the description is, of course, more complicated).

The geometry of a spherical bilayer is characterized by three independent parameters; for example, the outer radius R_C, the inner radius R_A and the radius of the effective boundary between inner and outer layers, R_B [1,12] (Fig. 1). It is important to recognize that all three must be determined independently, certainly on the same sample, and preferably at the same time. If only one or two are measured and the others taken arbitrarily, or from the intrinsically different planar bilayer system (e.g., assuming that $R_C - R_B$ equals $R_B - R_A$, or that the surface area per head group is the same in inner and outer layers, or that $R_C - R_A$ is already known), the question of asymmetry has been begged.

A complete description also requires the values for the molar volume of a phospholipid molecule in the inner and outer monolayers. These are similar, and, as a first approximation, we will take them as equal, and calculable from the apparent specific volume v (the total change in v for the gel-liquid crystal transition is only 5% [1] and differences here are a fraction of that). The phospholipid molecules can thus be visualized as filling truncated hexagonal pyramidal cells in inner and outer layer honeycombs. Even without knowing R_C, R_B and R_A one can see that the packing of the hydrocarbon chains in the inner and outer layers is intrinsically different: the tail region in the outer pyramid is the narrow base, while it is the broad base of the inner pyramid.

Three parameters more directly related to observable quantities are: x, the ratio of the number (N) of dipalmitoyl phosphatidylcholine molecules in the outer monolayers to that in the inner monolayers; y^3, determined from the

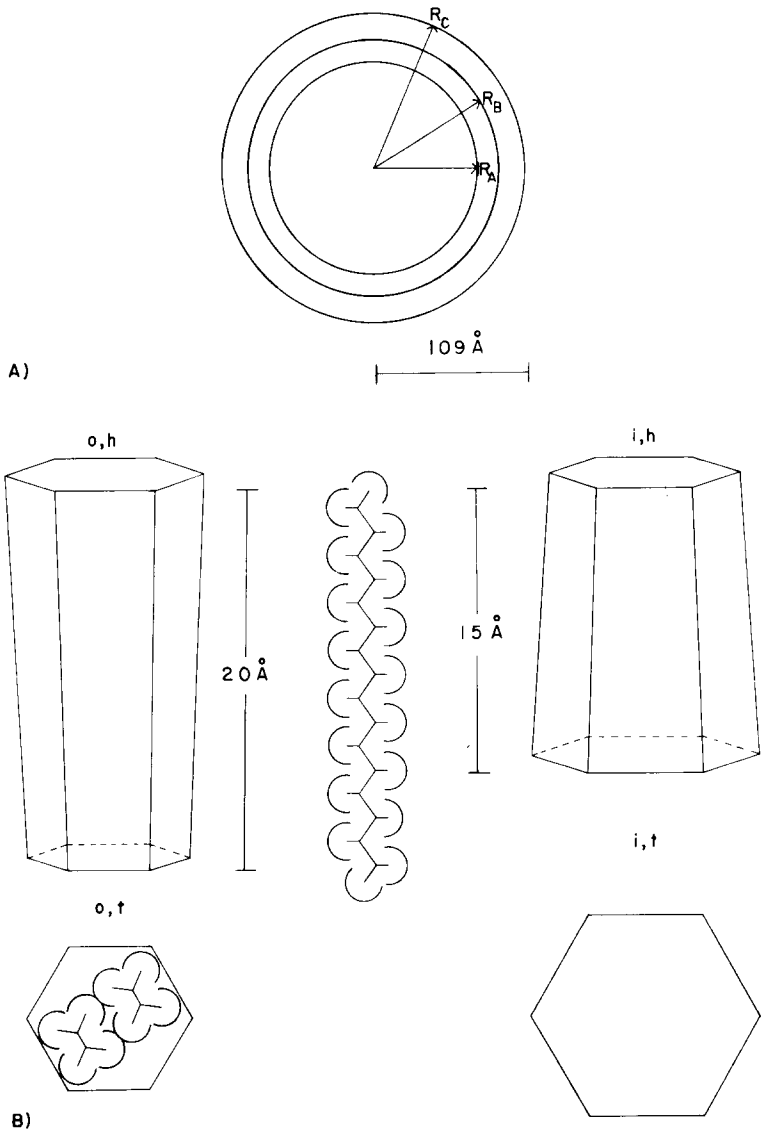

Fig. 1. (A), diagram of dipalmitoyl phosphatidylcholine bilayer vesicle with the radii R_A, R_B and R_C drawn to relative scale. (B), expanded drawings of the molecular unit cells of each monolayer with the notation, o,h, o,t, i,h, i,t, denoting outer monolayer head group, outer monolayer tail, inner monolayer head group and inner monolayer tail, respectively. Also, a single all-*trans* hydrocarbon chain is shown, drawn to the same scale, as a cross-section in the plane of the 16-carbon backbone with appropriate lengths for projected C-H bonds and Van der Waals radii. The relative areas of the two tail ends (at R_B) are depicted by the two hexagons. The projections of two all-*trans* chains are superimposed on the outer monolayer tail area for comparison.

volume of phospholipid, V_{DPPC} *, and of enclosed solvent, V_{IN}; and M, the vesicle particle weight. These parameters, being functions of (length)^3, also give smaller errors in the determinant volumes than parameters that are linear in length.

* DPPC, dipalmitoyl phosphatidylcholine.

$$x \equiv \frac{N_{DPPC,OUT}}{N_{DPPC,IN}} = \frac{(R_C^3 - R_B^3)}{(R_B^3 - R_A^3)} \quad (1)$$

$$y^3 \equiv \frac{(V_{DPPC} + V_{IN})}{V_{IN}} = \frac{R_C^3}{R_A^3} \quad (2)$$

$$M = N_{Avog} \frac{4}{3}\pi \frac{(R_C^3 - R_A^3)}{\bar{v}} \quad (3)$$

The quantities x and y^3 are determined simultaneously by ^{31}P magnetic resonance spectroscopy; $<M/R_S>_w$ (where R_S is the hydrodynamic (Stokes) radius) is determined in parallel, on the same solutions, by velocity ultracentrifugation. *

The L-α-dipalmitoyl phosphatidylcholine bilayer vesicles were prepared by sonicating ≈8% suspensions of dipalmitoyl phosphatidylcholine in ^2H_2O under nitrogen, for 20—30 min at a temperature above 42°C, the phase transition temperature, in the presence of a water-soluble solute, sodium dimethyl phosphate. The chosen conditions minimize fusion of small vesicles [9,14] and produce fairly narrow size distributions, without significant ultrasonic damage to the phospholipid [9]. The centrifuged clear solutions were analyzed for phosphate to determine the final dipalmitoyl phosphatidylcholine and Me_2P^- ** concentrations [15]. Densities were determined pycnometrically.

A small amount of Pr^{3+} is added to the solution. Rapid exchange of Pr^{3+} with external dipalmitoyl phosphatidylcholine and Me_2P^- moves the ^{31}P chemical shifts of these species downfield by the weighted average of shifts of free and complexed species appropriate to the given concentration of Pr^{3+} [12] (Fig. 2). Since Pr^{3+} does not penetrate into the vesicle inner space for days, as is clear from the NMR spectra, the ^{31}P chemical shifts of inner monolayer dipalmitoyl phosphatidylcholine and enclosed Me_2P^- remain undisturbed.

The ^{31}P NMR spectra were obtained at 52°C, on a Varian XL-100 NMR spectrometer, in Fourier transform mode, using a 90° pulse (41 μs) and pulse delays of 100—125 s. So that areas under the respective peaks correspond exactly to relative concentrations of inner and outer dipalmitoyl phosphatidylcholine and Me_2P^-, note must be taken of differential saturation (T_1) and Nuclear Overhauser Enhancement effects. Dipalmitoyl phosphatidylcholine, with a short T_1, presents no problem in this respect. However, T_1 for Me_2P^- is long and considerably shortened on the outside by interaction with Pr^{3+} [12]; therefore, intervals between pulses were taken as 5 times the longest T_1. Differences in Nuclear Overhauser Enhancement for ^1H decoupled spectra are not negligible, either for inner vs. outer dipalmitoyl phosphatidylcholine or Me_2P^-. This problem is avoided by taking undecoupled spectra, even tough integration of the resulting septuplets of Me_2P^- is more difficult. The quantity x is the

* In principle, all three parameters can be determined simultaneously from the ^{31}P NMR spectrum. Recent results indicate that the linewidth of the phospholipid resonance is proportional to $<R_S>^3$ [13]. However, since the proportionality constant cannot be calculated (it depends on temperature, viscosity and magnetic field strength) but must be calibrated, we have elected the more direct measurement of $<M/R_S>$ by ultracentrifugation.

** Me_2P^-, dimethyl phosphate.

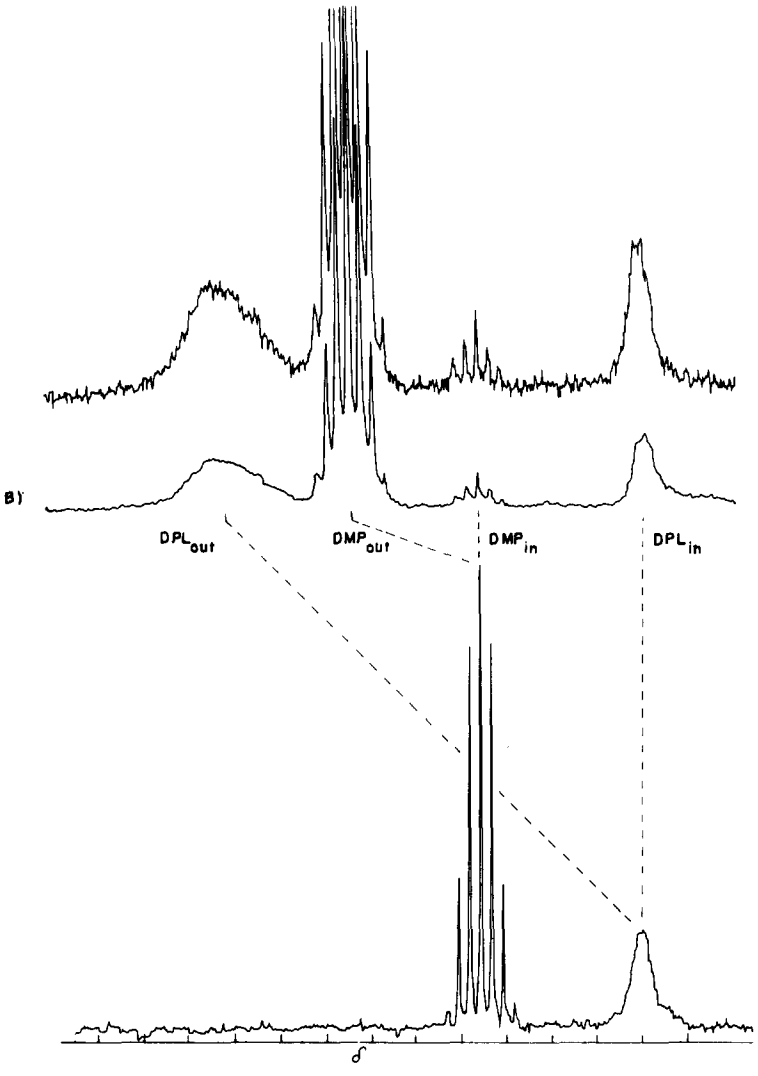

Fig. 2. (A), a ^{31}P NMR spectrum of dipalmitoyl phosphatidylcholine (DPL) bilayer vesicles and sodium dimethy phosphate (DMP) in $^{2}H_2O$ at 52°C. (B), spectrum of same solution with $Pr(NO_3)_3$ added.

ratio of intensities of downfield (outer) to upfield (inner) dipalmitoyl phosphatidylcholine resonances (i.e., the relative areas in Fig. 2), while y^3 is obtained from $R_{O/I}$, the ratio of intensities of outer to inner Me_2P^- resonances, by

$$y^3 = (1 + \overline{v}\, C_{DPPC} R_{O/I})/(1 - \overline{v}\, C_{DPPC}) \tag{4}$$

where C_{DPPC} is in g/ml. A typical solution with C_{DPPC} = 0.053 M gave $R_{O/I}$ = 38 and thus, y^3 = 3.2. (Anomalously low values of $R_{O/I}$ were obtained when Nuclear Overhauser Enhancement effects were not avoided [12].)

As in all solute-partitioning determinations of compartment volumes, it is assumed (hoped) that binding of the solute to the walls of the compartment, as well as closest-approach excluded-volume effects, are negligible. The mea-

sured values of T_1 for inner Me_2P^-, outer Me_2P^- (in the absence of added Pr^{3+}), and in solutions of $NaMe_2P$ alone, are 23 ± 1, 23 ± 1, and 22 ± 1 s, respectively, indicating, first, that Me_2P^- does not bind significantly to either side of the dipalmitoyl phosphatidylcholine bilayer, and second, that the water inside the vesicle behaves like bulk water. There may be a small decrease in y^3 with increasing (Me_2P^-), a trend we are continuing to investigate; the effect is consistent with the observed decrease of $\langle R_C \rangle$ with increasing ionic strength [1].

Sedimentation, or rather flotation, in the ultracentrifuge was used to obtain $\langle M/R_S \rangle_w$, from the Svedberg equation (s^0 is the sedimentation coefficient at zero concentration, ρ is density, and η is viscosity)

$$s^0 = \left\langle \frac{M}{R_S} \right\rangle_w \cdot \frac{(1 - \bar{v}\rho)}{6\pi\eta N_{Avog}}$$

assuming $\bar{v}$ = 0.985 ml/g [16], for vesicles above the transition temperature. The use of ^2H_2O makes $|(1 - \bar{v}\rho)|$ larger and less sensitive to errors in $\bar{v}$. The temperature, out of timidity, was 45°C. There was one major peak, with a typical value of $\langle M/R_S \rangle_w$ of $2.05 \cdot 10^4$ daltons/Å, and either some asymmetry or a minor peak attributable to unfused dimers [9]. The slight dependence of s on dipalmitoyl phosphatidylcholine concentration [17,18] can be taken into account; given the limitations of the perfect sphericity assumption it is perhaps excessive to make a distinction between R_C and R_S, the radius of the surface of shear, but one can, not entirely arbitrarily, include a monolayer of water molecules, or 3 Å, in the radius of the kinetic species [17]. These modifications do not greatly affect out conclusions.

Our results are summarized in Table I. The values given are for a median solution. The ranges in parentheses result, at least in part, from trends (related values of, e.g. $\langle R_C \rangle$ and $\langle R_A \rangle$ are correlated and the important differences, $R_C - R_A$, $R_C - R_B$, and $R_B - R_A$, are known with reasonable precision). The value of $\langle R_C \rangle_n$, 109 Å, is in excellent agreement with a quasi-elastic light scattering value, 110 Å, for dipalmitoyl phosphatidylcholine vesicles [9] and not far from the less direct gel filtration value, 125 Å [1]. Hydrodynamic

TABLE I

GEOMETRIC AND MOLECULAR PACKING PARAMETERS OF DIPALMITOYL PHOSPHATIDYLCHOLINE BILAYER VESICLES DETERMINED VIA EQNS. 1–3

Parameters	Median value *	(Range)
	(Å)	
R_C	109	(105–113)
$R_C - R_B$	19.8	(18–21.6)
$R_B - R_A$	15.2	(13.5–16.9)
	($Å^2$)	
$A_{o,h}$	75.6	(70.8–80.4)
$A_{i,h}$	67.9	(58.2–77.5)
$A_{o,t}$	50.8	(45.0–56.5)
$A_{i,t}$	97.6	(89.6–105.7)

* Solutions varied from 0.062 M to 0.104 M in dipalmitoyl phosphatidylcholine and from 0.090 M to 0.176 M in sodium dimethyl phosphate. Thus, a median value, rather than an average value from all experiments, is given. Note that individual experimental values are averages and that the trends in lengths and areas are the same, e.g. $A_{o,h} > A_{i,h}$, in each experiment.

values for egg phosphatidylcholine vesicles in solution are similar (see refs. 17 and 18 for examples). Electron microscope determinations using negative staining, which are known to be overestimates, are somewhat larger [1,16].

The average thickness, $<R_C - R_A>_n$, of 35 Å, is in excellent agreement with the egg phosphatidylcholine value of 37 Å [17], obtained from sedimentation coefficients and the ^{42}K and ^{24}Na "spaces". Another value, 53 Å, obtained from the ferricyanide "space" [18], seems extraordinarily thick. While the last result may arise partly from the distance-of-closest-approach excluded-volume effect, for the large $Fe(CN)_6^{3-}$ sphere, we feel that the discrepancy probably arises from loss of $Fe(CN)_6^{3-}$ during gel filtration, from vesicle breakage and reformation by interaction with lipid adsorbed by the Sepharose 4B (see discussion in ref. 17). The Me_2P^- inner and outer spaces are, of course, determined in situ, without need for separation. X-ray diffraction studies of planar dipalmitoyl phosphatidylcholine bilayers above the transition temperature give values of 35 Å [19] or 36 Å [20] for peak to peak headgroup separation, with a hydrocarbon layer thickness of at least 28 Å. Comparable values for egg phosphatidylcholine planar bilayers are 37 Å and 31 Å [21,22]. Below the transition temperature, the thickness increases by perhaps 10 Å [19].

We have now reached the central point of this report. From the value of x, 1.90 (which agrees with values obtained from careful ^1H, ^{13}C, and ^{31}P studies where T_1 and Nuclear Overhauser Enhancement problems were taken into account; see ref. 12 for references) and the values of $<R_C>_n$ and $<R_A>_n$, the average thickness of the outer and inner layers of the bilayer can be calculated. The inner layer is significantly thinner than the outer layer: 15 Å compared to 20 Å. This result has also been suggested by recent X-ray diffraction studies of sonicated dipalmitoyl phosphatidylcholine vesicles (Webb, N.G., unpublished). The inner dipalmitoyl phosphatidylcholine truncated pyramid is, therefore, much squatter with an average head group end area of 68 $Å^2$ at R_A and an area of 98 $Å^2$ at R_B, while the outer cell has areas of 76 $Å^2$ in the head region at R_C and 51 $Å^2$ in the tail region at R_B. (The average surface area per headgroup reported [17], for small egg phosphatidylcholine vesicles, corresponds exactly to the weighted average of our values for the two surfaces). Comparable values for cylindrical packing in planar egg phosphatidylcholine structures are 61 $Å^2$ (monolayers, by surface pressure measurements [22]) and 62.7 $Å^2$ (bilayers, by X-ray diffraction [21].

In principle, for planar bilayers and cylindrical molecular cell geometries, a monolayer can be thinned and the effective surface area for both tail and head ends increased, either by shortening and thickening the cylindrical cell, or by tilting the cylinder axis away from the normal to the surface plane. Given that the axial cross-section of all-*trans* alkyl chains is not much more than 30 $Å^2$ [23], it is likely even a priori that folding, rather than tilting, is primarily responsible for the 62 $Å^2$ effective cross-section and equivalent shortening, observed for the cells in planar bilayers above the transition temperature. In any case, for the truncated prismatic cell in small vesicles, the required smooth increase in cross-section along a vesicle radius (68 $Å^2$ (head) → 98 $Å^2$ (tail) inner cell; 51 $Å^2$ (tail) → 76 $Å^2$ (head) outer cell) cannot be produced by tilting.

In fact, regardless of whether or not there are measurable differences in average disorder between planar (or multilamellar) bilayers and curved (small

vesicle) bilayers above the transition temperature [5], it is clear that the gel-to-liquid crystalline transition does produce a major shift from essentially *trans* to significantly *gauche* orientations along the carbon skeletons of the lipid chains in all systems [2,6,23]. However, from our results the distribution of kinks and/or bends is clearly different in each monolayer. Truncated prismatic cells are, of course, abstractions but what must be borne in mind is that the equilibrium density of the lipid molecular cells must be satisfied over both time and space, so that while individual chains may wander out of specific cells or penetrate the other layer, an instantaneous snapshot will show almost all chains conforming to the required density, and thus to the required packing geometry. Neither equilibrium tilting nor its dynamic equivalent, wagging of all-*trans* tails, can satisfy the density or packing criteria. The hydrocarbon chains in the longer cells of the outer monolayer, with excess surface at the head end and narrower tail ends, have fewer kinks which, to fill the volume, must be distributed more toward the head end than the tail end, although some hairpin-like folding will give a similar effect. Chains in the cells of the inner monolayer have raidal projections of not more than 10—12 Å (the head occupies some space), not much over half the length of an all-*trans* palmitate chain, and must cover a large tail area; there must be more *gauche* configurations and the probability of kinks and bends must increase toward the CH_3 end. Thus, we can visualize both the 5 Å length difference and the nearly doubled tail area (Fig. 1), to be equivalent to an average gain of two 2g1 kinks [23] for the inner monolayer chains with a concomitant loss of two 2g1 kinks for the outer chains.

Consistent with the near-equivalence of vesicle inner-layer and planar-layer head group areas is the observation that the ^1H NMR chemical shifts of such choline methyl group resonances are similar, while that of the outer $-N(CH_3)_3$ is shifted, and more sensitive to temperature and salt effects [1]. NMR studies of various ^{19}F-substituted lipids demonstrating both environmental (chemical shift) and dynamic (T_2) differences between chain loci in inner and outer layers of small vesicle bilayers, in the directions implied by the asymmetry reported here, are being completed (ref. 24 and Dahlquist, F.W., personal communication).

Finally, we note that the method discussed here is indispensable to a proper NMR analysis of component distribution in each layer of mixed-lipid bilayers: changes in x alone cannot distinguish unequal distribution of components from changes in vesicle size parameters. Our results show that there is an inherent, asymmetric molecular packing of lipid molecules in the two monolayers of a curved bilayer, even when composed of a single type of phospholipid.

Acknowledgements

We would like to thank N.G. Webb and F.W. Dahlquist for kindly making available their unpublished results. One of us (CSS) would also like to thank Sunney Chan, Nils Petersen, and Bill Croasmun for many interesting and stimulating discussions. Finally, we would like to thank the National Institutes of Health for Biomedical Sciences Support Grant No. 31-H056C and Biomedical Research Support Grant No. 31-H071E (old No. 31-H071D) and the National

Science Foundation for Grants No. PCM75-14788A01 (old No. BMS75-14788) and No. PCM7600193.

References

1 Sheetz, M.P. and Chan, S.I. (1972) Biochemistry 11, 4573—4581
2 Mendelsohn, R., Sunder, S. and Bernstein, H.J. (1976) Biochim. Biophys. Acta 419, 563—569
3 Stockton, G.W., Polnazek, C.F., Tulloch, A.P., Hassan, F. and Smith, I.C.P. (1976) Biochemistry 15, 954—966
4 De Kruijff, B., Cullis, P.R. and Radda, G.K. (1975) Biochim. Biophys. Acta 406, 6—20
5 Gaber, B.P. and Peticolas, W.L. (1977) Biochim. Biophys. Acta, in press
6 Spiker, R.C. and Levin, I.W. (1976) Biochim. Biophys. Acta 455, 560—575
7 Lentz, B.R., Barenholz, Y. and Thompson, T.E. (1976) Biochemistry 15, 4529—4537
8 Lentz, B.R., Barenholz, Y. and Thompson, T.E. (1976) Biochemistry 15, 4521—4528
9 Suurkuusk, J., Lentz, B.R., Barenholz, Y., Biltonen, R. and Thompson, T.E. (1976) Biochemistry 15, 1393—1401
10 Spiker, R.C. and Levin, I.W. (1976) Biochim. Biophys. Acta 433, 457—468
11 Linden, C.D. and Fox, C.F. (1975) Acc. Chem. Res. 8, 321—327
12 Chrzeszczyk, A., Wishnia, A. and Springer, C.S. (1976) ACS Symp. 34, 483—498
13 De Kruijff, B., Cullis, P.R. and Radda, G.K. (1976) Biochim. Biophys. Acta 436, 729—740
14 Lawaczeck, R., Kainosho, M. and Chan, S.I. (1976) Biochim. Biophys. Acta 443, 313—330
15 Chen, P.S., Toribara, T.Y. and Warner, Huber (1956) Anal. Chem. 28, 1756—1758
16 Huang, C.-H. (1969) Biochemistry 8, 344—352
17 Johnson, S.M. (1973) Biochim. Biophys. Acta 307, 27—41
18 Newman, G.C. and Huang, C.-H. (1975) Biochemistry 14, 3363—3370
19 Janiak, M.J., Small, D.M. and Shipley, G.G. (1976) Biochemistry 15, 4575—4580
20 Cain, J., Santillan, G. and Blasie, J.K. (1972) in Membrane Research (Fox, F., ed.), Vol. 1, pp. 3—14, Academic Press, New York
21 Levine, Y.K. and Wilkins, M.F.H. (1971) Nat. New Biol. 230, 69—72
22 Fettiplace, R., Andrews, D.M. and Haydon, D.A. (1971) J. Memb. Biol. 5, 277—296
23 Lee, A.G. (1975) Prog. Biophys. Molec. Biol. 29, 3—56
24 Longmuir, K.J. and Dahlquist, F.W. (1976) Proc. Natl. Acad. Sci. U.S. 73, 2716—2719